Passive Aeroelastic Tailored Wing Modal Test Using the Fixed Base Correction Method

Natalie Spivey[1], Rachel Saltzman[1], Carol Wieseman[2], Kevin Napolitano[3], Benjamin Smith[4]

[1] Armstrong Flight Research Center
National Aeronautics and Space Administration
4800 Lilly Ave Edwards, CA 93523 USA

[2] Langley Research Center
National Aeronautics and Space Administration
1 NASA Dr., Hampton, VA 23666 USA

[3] ATA Engineering, Inc
13290 Evening Creek Drive South, Suite 250, San Diego, CA 92128 USA

[4] Aurora Flight Sciences
2600 Paramount Pl, Suite 400, Fairborn, OH 45324

ABSTRACT
In modal testing and finite element model correlation, analysts desire modal results using free-free or rigid boundary conditions to ease comparisons of test versus analytical data. It is often expensive both in cost and schedule to build and test with boundary conditions that replicate the free-free or rigid boundaries. Static test fixtures for load testing are often large, heavy, and unyielding, but do not provide adequate boundaries for modal tests because they are dynamically too flexible and often contain natural frequencies within the frequency range of interest of the test article. Dynamic coupling between the test article and test fixture complicates the model updating process because significant effort is required to model the test fixture and boundary conditions in addition to the test article. If there were a way to correct the modal results for fixture coupling, then setups used for other structural testing could be adequate for modal testing. In the case described in this paper, a partial static loads testing setup was used, which allowed significant schedule and cost savings by eliminating a unique setup for a modal test. A fixed base correction technique was investigated during modal testing of a flexible wing cantilevered from part of a static test fixture. The technique was successfully used to measure the wing modes de-coupled from the dynamically active test fixture. The technique is promising for future aircraft applications, but more research is needed.

Keywords: Modal Test, Ground Vibration Test, Fixed Base, Passive Aeroelastic Tailored Wing

NOMENCLATURE

a	=	acceleration
accel	=	accelerometer
AFRC	=	Armstrong Flight Research Center
CFAST	=	a NASTRAN element that connects two shell elements to provide the joint stiffness of the connecting elements

CReW = Calibration Research Wing
DOF = degrees of freedom
f = external force
fwd = forward
FBC = Fixed Base Correction
FEM = finite element model
FLL = Flight Loads Laboratory
FRF = frequency response function
GVT = ground vibration test
Hz = Hertz
iso = isometric
k = structural stiffness
lb = pound
LE = leading edge
m = mass
MAC = modal assurance criterion
MIF = Mode Indicator Function
NASA = National Aeronautics and Space Administration
NMIF = Normal Mode Indicator Function
OML = outer mold line
PAT = Passive Aeroelastic Tailored
PSMIF = Power Spectrum Mode Indicator Function
TE = trailing edge
W1B = wing 1st bending
W2B = wing 2nd bending
W3B = wing 3rd bending
W4B = wing 4th bending
W5B = wing 5th bending
W6B = wing 6th bending
W7B = wing 7th bending
W1T = wing 1st torsion
W2T = wing 2nd torsion
W1F/A = wing 1st fore/aft
W2F/A = wing 2nd fore/aft
W3F/A = wing 3rd fore/aft
W4F/A = wing 4th fore/aft
WLTF = Wing Loads Test Fixture
x = displacement
ω = frequency

1 INTRODUCTION

New aircraft structures often require static and dynamic structural ground testing to validate the analytical structural finite element models (FEMs) used in determining airworthiness. Static and dynamic ground tests require different boundary conditions, which result in two different costly and specialized test setups. Therefore, it would be beneficial if a modal survey could be conducted while a test article is mounted in a static test fixture for a structural loads test, allowing for two traditionally separate structural tests to be performed using one test fixture. This paper discusses an effort to apply a fixed base correction technique to measure fixed base modes from a test article mounted to part of a dynamically active static test fixture.

The Flight Loads Laboratory (FLL) at the National Aeronautics and Space Administration (NASA) Armstrong Flight Research Center (AFRC) (Edwards, California) specializes in both structural modal testing and loads calibration testing of aerospace research structures.[1] To facilitate the loads calibration test on the Passive Aeroelastic Tailored (PAT) Wing, a Wing Loads Test Fixture (WLTF), shown in figure 1, was designed.

The PAT Wing - a carbon-epoxy high-aspect-ratio wing of an approximately 39-ft semi-span - was built to investigate a new composite technology known as tow-steering to increase aeroelastic efficiencies [2-4] and underwent a modal test in the FLL. The modal test of the high-aspect-ratio, tow-steered wingbox was conducted to validate the FEM. The objective of the modal test was to measure the primary frequencies, mode shapes, and damping up to the Wing 1st Torsion (W1T) mode (expected to be approximately 55 Hz). To streamline the modal test and save significant project resources of time, cost, and schedule, the modal test used the same hardware configuration as was used for the follow-on loads testing, with the wing cantilevered out from the WLTF table. This setup differs from a standard modal test setup. The boundary conditions of the wing mounted onto the WLTF table were not ideal for modal testing because truly rigid boundary conditions were not required for static loads testing. Finding the analytical connection stiffness of how the wing was physically mounted would be a very difficult analytical task; however, by using the Fixed Base Correction (FBC) test method, the table-mounted boundary conditions were analytically fixed for the modal test.

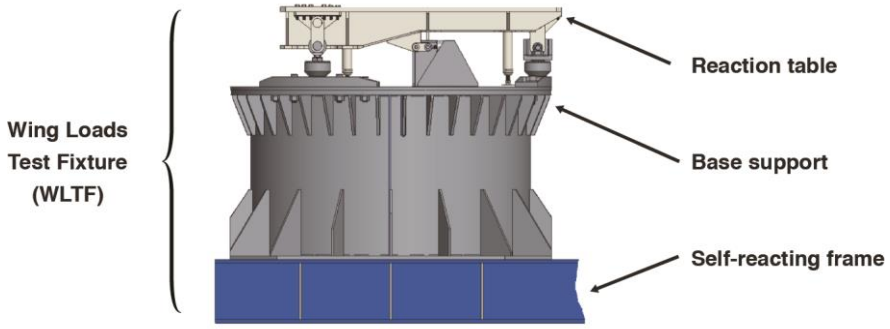

Figure 1: Side view of the dynamically active static Wing Loads Test Fixture

The uniqueness of FBC methodology compared to traditional modal tests is that it requires an equal number of independent drive point inputs (that is, shakers) as base mode shapes to remove. The result is that many shaker inputs are required; the number depends on the complexity of the base which is desired to be "fixed." The FBC method allows for test articles to be tested with non-ideal modal testing boundary conditions that can normally complicate testing and drive up cost and schedule. While a traditional ground vibration test (GVT) only requires shakers be attached to the wing or test article, the FBC method also requires multiple shakers be attached to the mounting fixture. The fixture excitation accelerations are used as references when calculating frequency response functions (FRFs) instead of using the traditional shaker forces as references. This FBC strategy analytically removes and de-couples enough of the fixture response from the wing in order to "fix" the fixture and aid in comparing modal ground test results to FEM modal results. More detail regarding the background of the FBC method is presented below. This paper details the second time that the FBC technique has been applied to aeronautics applications. The FLL previously conducted a test on the Calibration Research Wing (CReW); this was a pathfinder GVT for the PAT Wing test.[5] Using the CReW static loads testing setup for the GVT and implementing FBC allowed significant schedule and cost savings by eliminating a unique setup for a modal test.

2 THEORY / CORRECTION METHODOLOGY

There exists considerable literature discussing how to extract fixed base modes from structures, mainly satellite-related structures, mounted on shake tables.[6–14] These methods require two different approaches to extract fixed base modes from structures mounted on flexible shake tables. One method applies a constraint equation to measured mass-normalized mode shapes to generate fixed base modes.[15] The advantage of using mass-normalized modes is that a large number of shakers do not necessarily need to be mounted on the base, which simplifies the test setup. The accuracy of this method, however, depends on how well a linear combination of the measured modes can represent the fixed base modes. If the measured test modes don't span the space of the true

fixed base modes, then this method will not be able to accurately estimate them. The method also requires well-excited modes so that modal mass can be accurately calculated. A second method, hereafter called the Fixed Base Correction method, is the focus of this paper and uses base accelerations as references to calculate the FRFs associated with a fixed base.[16-17] The FRFs are then post-processed to extract fixed based modes of the test article.

The FBC method can be illustrated with a simple spring-mass 2-degrees-of freedom (2-DOF) system, as shown in Figure 2.

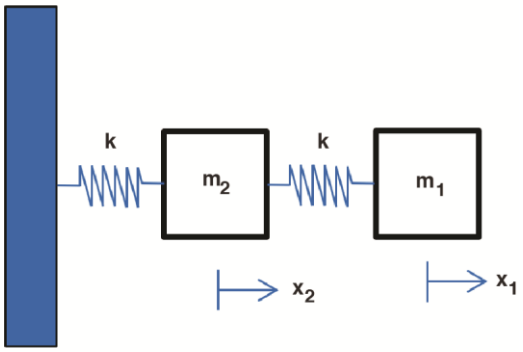

Figure 2: Spring-mass two-degrees-of-freedom system

Applying Newton's second law, the equation of motion for an undamped system in the frequency domain is as shown in eq. (1):

$$\begin{bmatrix} -\omega^2 m_1 + k & -k \\ -k & -\omega^2 m_2 + 2k \end{bmatrix} \begin{Bmatrix} x_1 \\ x_2 \end{Bmatrix} = \begin{Bmatrix} f_1 \\ f_2 \end{Bmatrix} \tag{1}$$

where m is the mass, ω is the frequency, k is the structural stiffness, x is the displacement, and f is the external force. The subscripts 1 and 2 refer to blocks 1 and 2, respectively. It should be noted that the 2-DOF system above is the same k value, but the FBC method can be further generalized for different structural stiffness values.

The FRF for traditional modal testing is calculated using the shaker forces applied to DOF 1 and DOF 2 as references to obtain the full system response. The results of using these traditional FRFs are referred to in this paper as the "uncorrected" results, as shown in eq. (2):

$$a_1 = \begin{bmatrix} \dfrac{-\omega^2(-\omega^2 m_2 + 2k)}{(-\omega^2 m_2 + 2k)(-\omega^2 m_1 + k) - k^2} & \dfrac{-\omega^2 k}{(-\omega^2 m_2 + 2k)(-\omega^2 m_1 + k) - k^2} \end{bmatrix} \begin{Bmatrix} f_1 \\ f_2 \end{Bmatrix} \tag{2}$$

where a is the acceleration.

When implementing the FBC, however, if the force at DOF 1 and the acceleration at DOF 2 are used as references, then the resulting FRFs are associated with a structural system with dynamics associated with DOF 2 fixed, as shown in eq. (3):

$$a_1 = \begin{bmatrix} \dfrac{-\omega^2}{-\omega^2 m_1 + k} & \dfrac{k}{-\omega^2 m_1 + k} \end{bmatrix} \begin{Bmatrix} f_1 \\ a_2 \end{Bmatrix} \tag{3}$$

Furthermore, the FRF associated with the force applied at DOF 1 is equivalent to an FRF associated with DOF 2 being fixed. This property is exploited in the FBC method by using drive point accelerations, instead of the traditionally used shaker forces, on the test fixture as references when calculating the FRF.

The key necessity of the FBC method is at least one independent excitation source, usually modal shakers, for each degree of freedom that is desired to be fixed. Therefore, FBC modal testing requires multiple shakers used on the test fixture in addition to the test article. Although not described in this paper, the FBC technique could also use constraint shapes as references when the number of independent sources is larger than the number of independent DOF of the test fixture.[16] The fundamental FBC strategy is to use shaker accelerations as references, rather than the traditional shaker forces, when calculating FRFs. Personnel at ATA Engineering, Inc. (San Diego, California) have implemented the FBC modal methodology into their IMAT™ (Interface between MATLAB®, Analysis and Test) software (MATLAB is a registered trademark of The MathWorks, Natick, Massachusetts).

The fixed base corrected FRF can be calculated directly using shaker accelerations on the fixture and shaker forces on the test article as references [18], or by performing a partial inversion of the baseline FRFs that have been calculated using all shaker forces as references.[6, 17] In fact, the results are equivalent if measured forces are used as basis vectors when calculating the FRF directly.[19]

One advantage of calculating the FRF directly is that doing so removes the requirement to mount load cells to the shakers on the test fixture. The advantage of performing a partial inversion of the FRF matrix is that boundary conditions can be changed quickly by changing which DOF are to be inverted.

One potential disadvantage of the FBC method is that the measured damping values of the FBC modes have been observed to be slightly different from expected values; sometimes very lightly damped modes may even be calculated to have slightly negative damping. In these cases, it may be better to report the damping values of the mode from the uncorrected test data that best align with the FBC mode. Analytically, the damping values calculated from the FBC method should be accurate. Further study is needed to understand how the FBC method affects damping measurements.

3 TEST DESCRIPTION

The following sections describe the PAT Wing test article, the finite element model, and the modal testing details. The PAT Wing modal testing was conducted in the summer of 2018 with the intent to use the FBC method.

3.1 Test Article

The PAT Wing test article, depicted in figure 3, is a carbon-epoxy, semi-span, flexible right wingbox designed and manufactured by Aurora Flight Sciences (Manassas, Virginia) (“Aurora”) using a composite technology called tow steering. The test article is a 27-percent scale model of the NASA undeflected Common Research Model (uCRM) with a high aspect ratio of 13.5, 36.8-degree wing sweep, and approximately 39-ft semi-span.

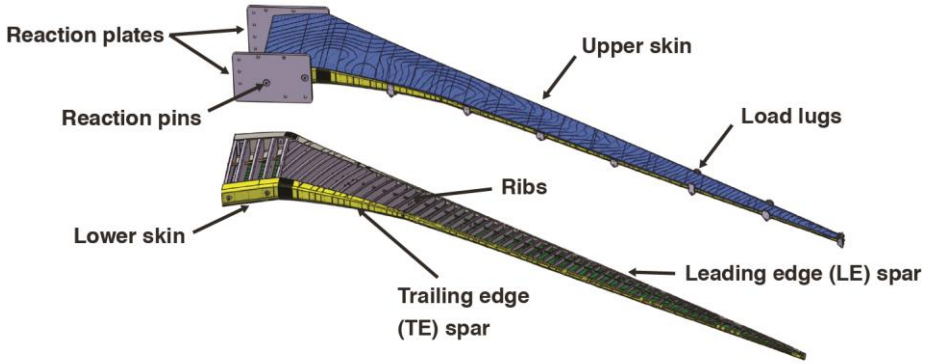

Figure 3: The Passive Aeroelastic Tailored Wing Test Article

The wingbox consists of two skins; both the upper and the lower surfaces are of the tow-steered wingskins. The forward and aft spars are primarily carbon-fiber composite. An outboard section of the forward spar was replaced with approximately 12 ft of aluminum due to manufacturing difficulties. The wing contains 58 composite ribs connected to the wingskins. Along the wingspan there are 14 load lugs: seven on the leading edge (LE) spar and seven on the trailing edge (TE) spar). The load lugs are permanently installed to the wingbox for the load testing; see figure 4. Along the TE spar there is a Yehudi break between lugs 1 and 2. At the wing root there are two large steel reaction plates (forward/LE and aft/TE) each containing two three-inch reaction pins. The root reaction plates are mounted to attachment hardware connecting to the WLTF table. The wingbox was assembled using numerous fasteners and, in some locations, bonding agents.

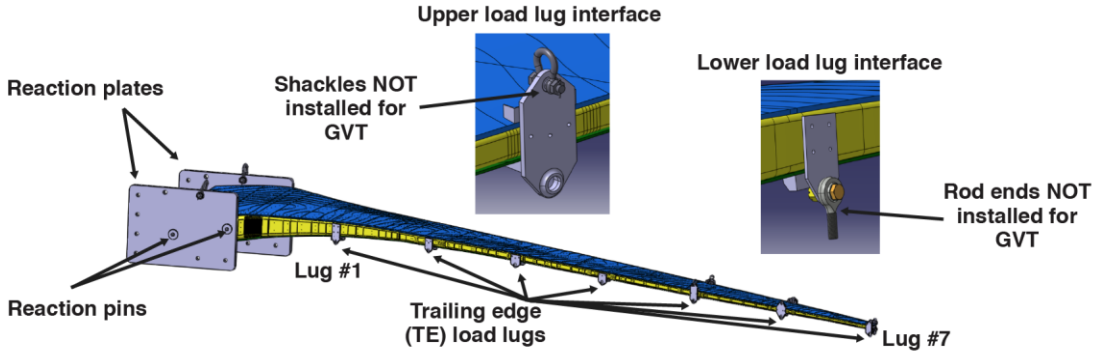

Figure 4: Load lugs on the leading edge and the trailing edge of the Passive Aeroelastic Tailored Wing

A weight and balance test was performed prior to the wing being shipped from Aurora to NASA AFRC. The wing weighed 2,621 lb with the installed reaction plates, the internal strain gage instrumentation, and the wire bundle.

While the root reaction plates are adequate for static testing because they carry static loads properly, they are not adequate for measuring fixed base modes because plates are dynamically flexible in the out-of-plane direction.

3.2 Finite Element Model

Data from both the modal and loads tests were used to validate the FEM analytical models, modeling techniques, and assumptions used for the towed-steering technology. Personnel of Aurora and of the NASA Langley Research Center (Hampton, Virginia) participated in a combined effort to create an MSC Nastran™ (MSC Software,

Newport Beach, California) FEM of the PAT Wing along with the wing reaction plates, attachment hardware, and WLTF reaction table, shown in figure 5. Unique material orientations were assigned to each wingskin element to account for the spatially varying tow-steering paths. Skins consisted of a laminate with 62.5 percent of the tows following the local tow-steering path and the balance of the laminate consisting of plies offset -45 deg, +45 deg, and 90 deg from the local tow-steering path. Homogenized laminate properties corresponding to this ply fraction were assigned to the skin elements based on unnotched tensile testing performed on representative tow-steering coupons.

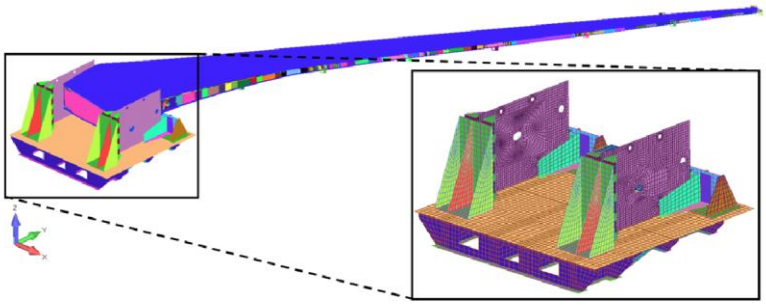

Figure 5: Finite element model of the Passive Aeroelastic Tailored Wing and the Wing Loads Test Fixture reaction table

The FEM modeled both rib and spar caps with shell elements, and fasteners were modeled utilizing discrete CFAST elements. Element offsets were applied to all skin elements to position them at the as-measured OML, which includes deviations from the nominal design due to local variations in liquid shim thickness between the skins and spar and rib caps in figure 6.

During the wing fabrication, some unexpected defects were found and multiple fixes were made to ribs and spars. Aurora subsequently updated the FEM to incorporate differences of the as-built wing. Non-structural masses were updated to account for as-measured part and assembly masses. This FEM was used for test predictions and post-test comparisons. Currently there are no plans to correlate the as-built FEM with test results.

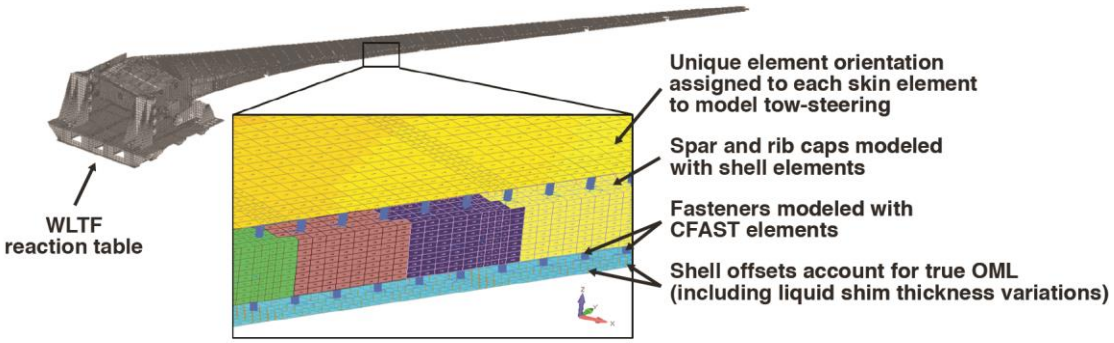

Figure 6: Finite element model of the Passive Aeroelastic Tailored Wing and the Wing Loads Test Fixture reaction table

3.3 Modal Test Setup

The PAT Wing modal test using the FBC method took place July 10-12, 2018 in the NASA AFRC FLL high bay. The original modal test setup plan for the FBC PAT Wing, shown in figure 7, was to perform the test with the wing installed on the dynamically active WLTF, as the wing would be for the loads testing. In this test configuration, the PAT Wingtip would be approximately 124 inches above the Flight Loads Laboratory floor.

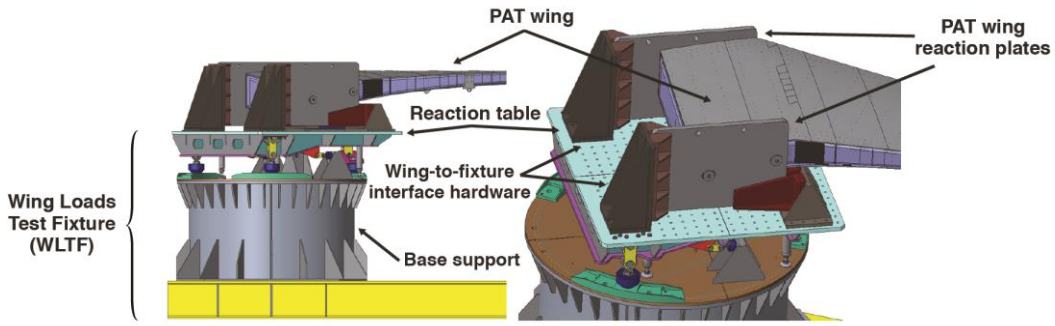

Figure 7: The original modal test setup plan: the Passive Aeroelastic Tailored Wing mounted on the Wing Loads Test Fixture

Upon further review of the test plan and understanding of the FBC technique, it was determined that the modal test could be simplified by setting the WLTF table directly on the FLL floor (see figure 8), rather than installing the reaction table on top of the WLTF base support. Using FBC made this approach possible because it analytically removed the effects of the reaction table and the hardware below it. The reaction table being set directly on the FLL floor also significantly simplified the shaker setup, because the wingtip now was only approximately 48 inches, rather than approximately 124 inches, above the FLL floor. This further simplification allowed cost savings by increasing access to the wing; attaching the shakers at lower heights also prevented adding additional flexibility and potential errors into the test. The reaction table on the FLL floor was supported by four retractable feet and secured with a strap to floor tracks as shown in figure 9. The wing was cantilevered from the reaction table by securing the two wing reaction plates to attachment hardware connected to the table.

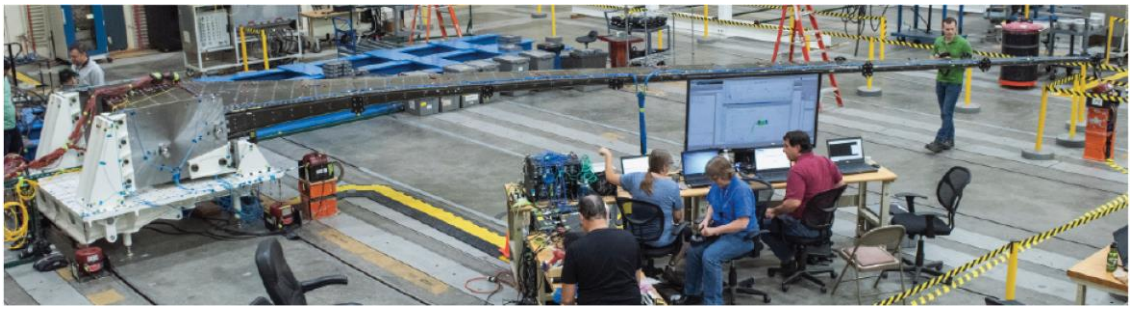

Figure 8: The simplified modal test setup: the Passive Aeroelastic Tailored Wing mounted on only the Wing Loads Test Fixture reaction table

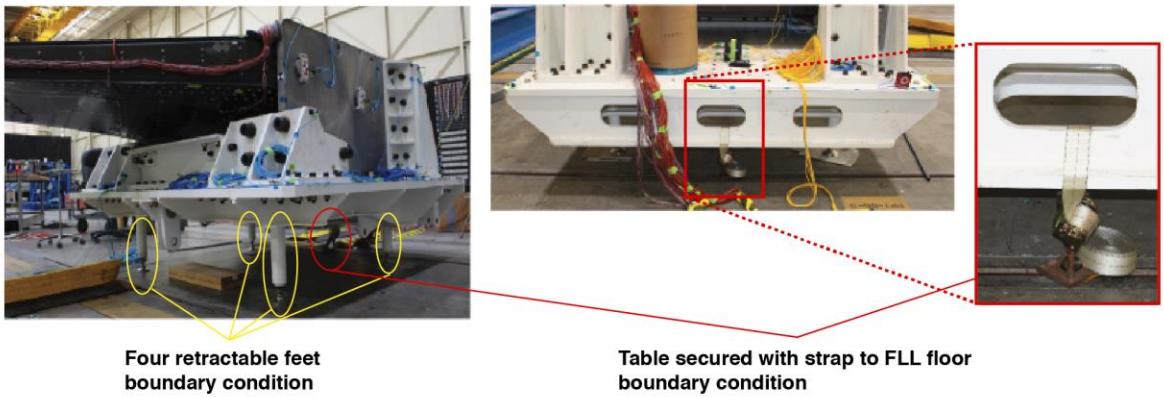

Figure 9: Boundary conditions of the Wing Loads Test Fixture reaction table on the Flight Loads Laboratory floor

3.4 Modal Test Instrumentation

Modal testing normally requires accelerometers with a sensitivity of 100 mV/g distributed over the test article and force transducers at the shaker locations. To implement the FBC method, additional 100 mV/g accelerometers were added on the hardware being fixed along with a small handful of seismic uniaxial accelerometers, which typically have a sensitivity of 1000 mV/g. The seismic accelerometers with the higher sensitivity were used at each shaker location on the hardware being fixed. This method produced clean shaker accelerometer data for use as references in the FBC method, as compared with traditional shaker forces being used as references for the FRFs.[15-16] The PAT Wing test used three different types of modal accelerometers (PCB Piezoelectronics, Depew, New York), shown in figure 10, depending on whether a uniaxial or triaxial accelerometer was desired to measure a certain number of DOF at each location along with the seismic accelerometers at the fixed shaker locations.

Figure 10: Ground test accelerometers used for modal testing (not to scale)

For every shaker attached to the reaction table or wing reaction plates, a reference seismic accelerometer in the direction of the shaker excitation along with a force transducer attached to the shaker stinger were used to measure the excitation input. Figure 11 shows an example of the seismic accelerometer and force transducer shaker setup that was used on the reaction table. The wingtip shaker did not require a seismic accelerometer and used a traditional modal accelerometer and force transducer because the force was used as a reference when calculating the FRF; see figure 12.

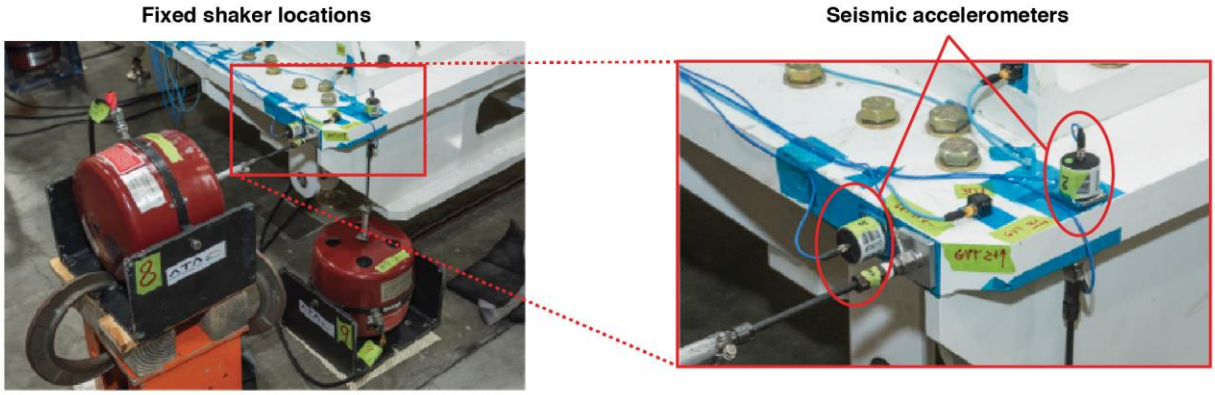

Figure 11: Typical shaker setup on the Wing Loads Test Fixture reaction table using seismic accelerometers

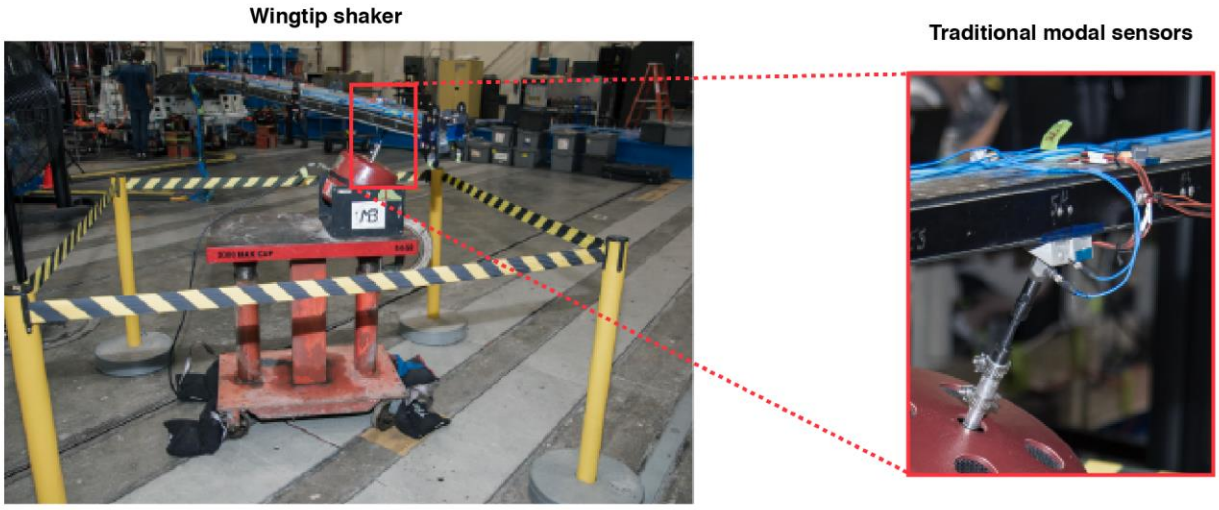

Figure 12: Wingtip shaker setup using traditional modal accelerometer and force transducer

3.5 Modal Test Accelerometer Layout

The PAT Wing modal test included accelerometers on the wing, as in traditional modal testing; implementing the FBC method required additional accelerometers on the WLTF reaction table, reaction plates, and the attachment hardware connecting them. The PAT Wing modal test used 106 different accelerometer locations for measuring a total of 274 DOF responses to acquire the desired mode shapes of the wing and test fixture needed to implement the FBC technique. The total included the accelerometer responses for the one wingtip shaker along with each fixed shaker location; these were later used as reference for the FBC. The data acquisition system also included the 14 shaker force transducers measured as references. Accordingly, a total of 288 channels were recorded with the data acquisition system for each test run.

Of the 106 total locations there were 31 accelerometer locations on the wing (see figure 13), which had triaxial accelerometers to measure a total of 87 DOF for the wing. The placement of the wing accelerometers was the same as for any traditional modal test; sensors should be placed to adequately observe and differentiate modes of the structure.

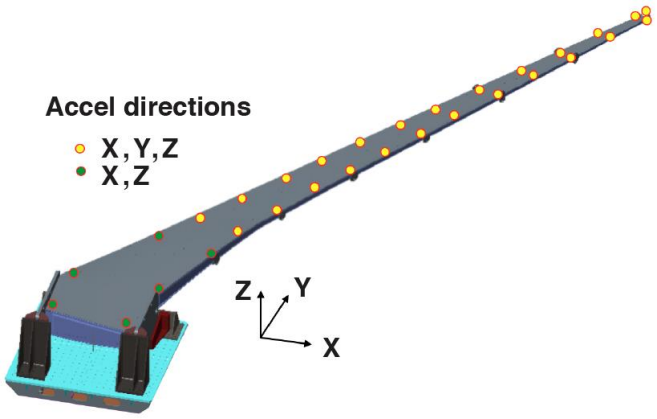

Figure 13: Accelerometer locations on the Passive Aeroelastic Tailored Wing

The remaining 75 locations were on the WLTF reaction table, attachment hardware, and the wing reaction plates to perform the FBC calculations. The majority of these locations used triaxial accelerometers for a total of 187 DOF measured on the hardware being fixed; see figure 14 (some accelerometer locations are not visible in the figure).

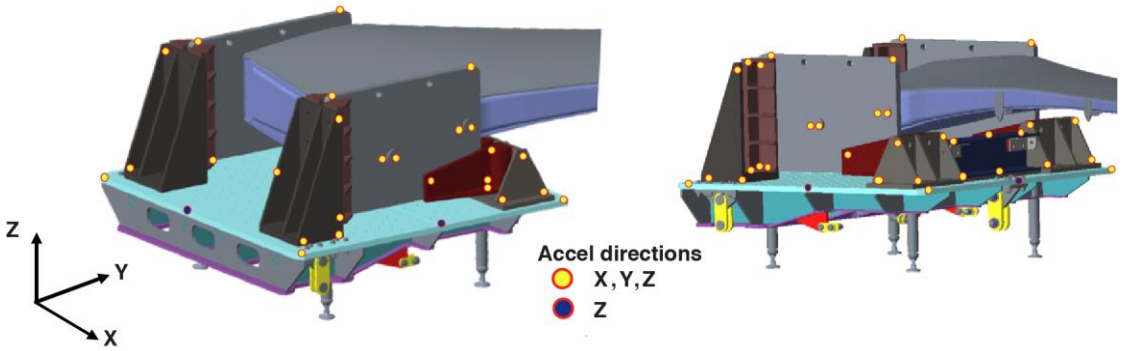

Figure 14: Accelerometer locations on the Wing Loads Test Fixture reaction table, attachment hardware, and wing reaction plates

The coordinates of the 106 accelerometer locations were used to create the test display model shown in figure 15. The test display model was used to visualize the test mode shapes.

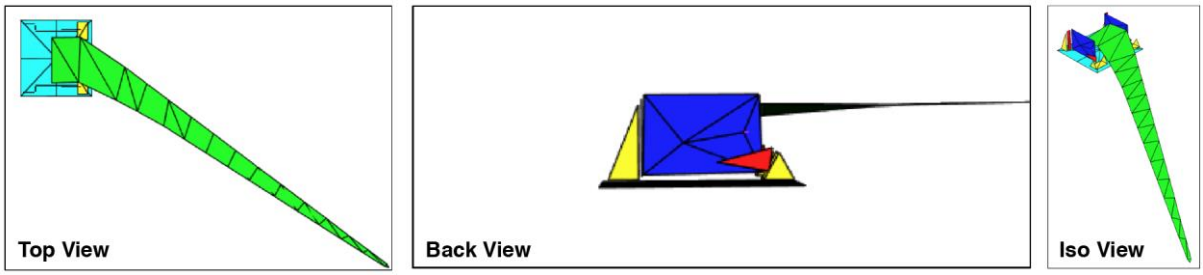

Figure 15: The Passive Aeroelastic Tailored Wing modal test display model

3.6 Modal Test Shaker Layout

The FBC technique requires multiple independent drive points (that is, shakers) be mounted to both the WLTF reaction table and the PAT Wing test article. The shaker layout depends on where the FBC technique is trying to fix the boundary conditions. There must be at least as many independent sources as there are independent boundary deformations of the hardware desired to be fixed in the test article frequency range of interest. The PAT Wing modal test included an effort to fix the reaction table by adding more shakers to improve the fixed base modes. For each shaker configuration, one shaker was always positioned on the wingtip as for traditional modal testing, and multiple other shakers were positioned around the WLTF reaction table and connecting attachment hardware.

During the PAT Wing modal test three different shaker configurations (see figure 16) were attempted with the FBC method to fix different hardware to improve the fixed base modes:

- 10 Shakers : nine shakers on the reaction table, one shaker on the wingtip
  - Vertical wingtip excitation
- 12 Shakers : two shakers added on aft triangular brackets (fore/aft)
  - Vertical wingtip excitation
- 14 Shakers : two shakers added on wing root reaction plates (fore/aft)
  - Vertical and fore/aft wingtip excitation

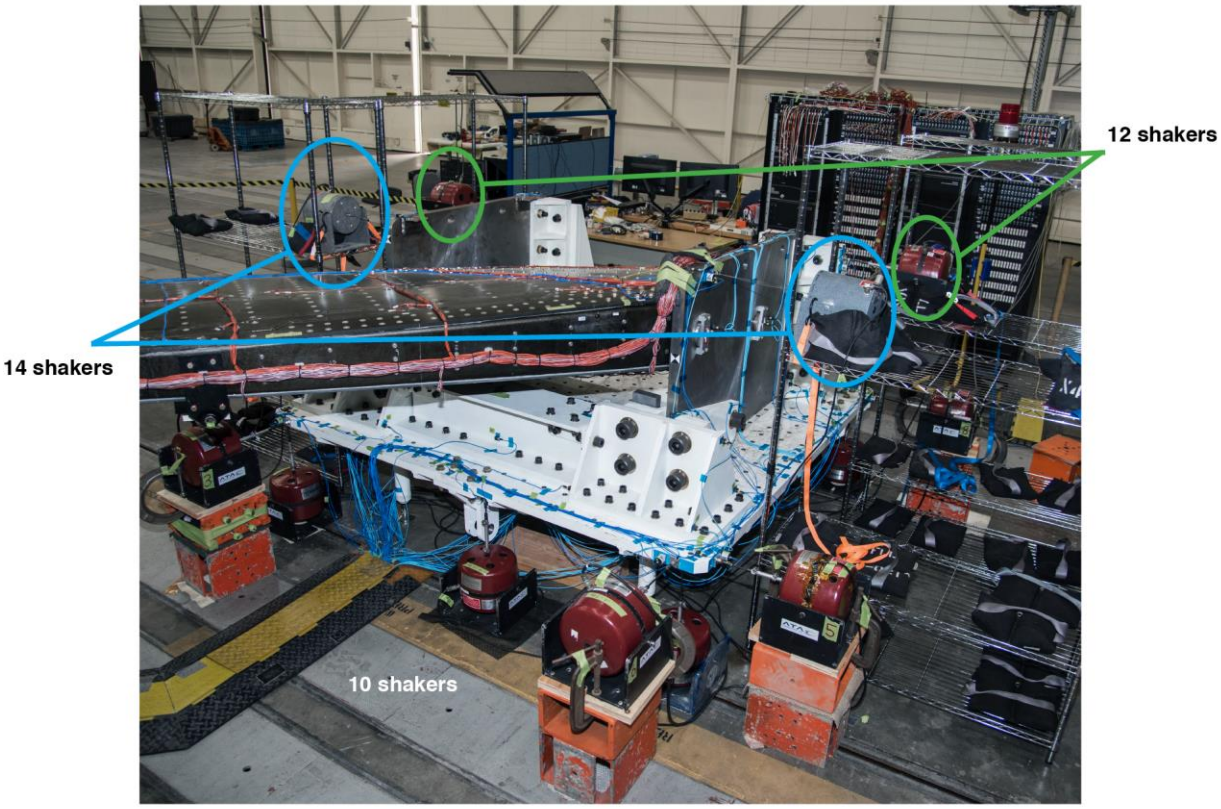

Figure 16: Shaker configurations on the Passive Aeroelastic Tailored Wing

The direction of the shakers on the reaction table and connecting hardware are important and essentially eliminate the effect of the hardware moving in each shaker direction; see figure 17. A few different shaker configurations were attempted to improve the fixed base modes to fix the reaction table. The final shaker layout consisted of 14 total shakers with one wingtip shaker plus 13 shakers around the reaction table and connecting hardware, as shown in figure 18. This method fixed the reaction table and connecting hardware enough to decouple the wing modes. The placement of the shakers around the WLTF was adjusted to excite primary base modes and maximize the capability of the FBC to decouple the base modes from the wing modes. The shakers used were MB Dynamics (Cleveland, Ohio) Modal 110-lb and Modal 50-lb electromagnetic shakers. Higher shaker forces were required on the base because it was stiffer than the wing which required less force at the wingtip. The wingtip shaker force was approximately 0.7 lb RMS for the various tests; the base shaker forces varied between 3 to 5 lb RMS.

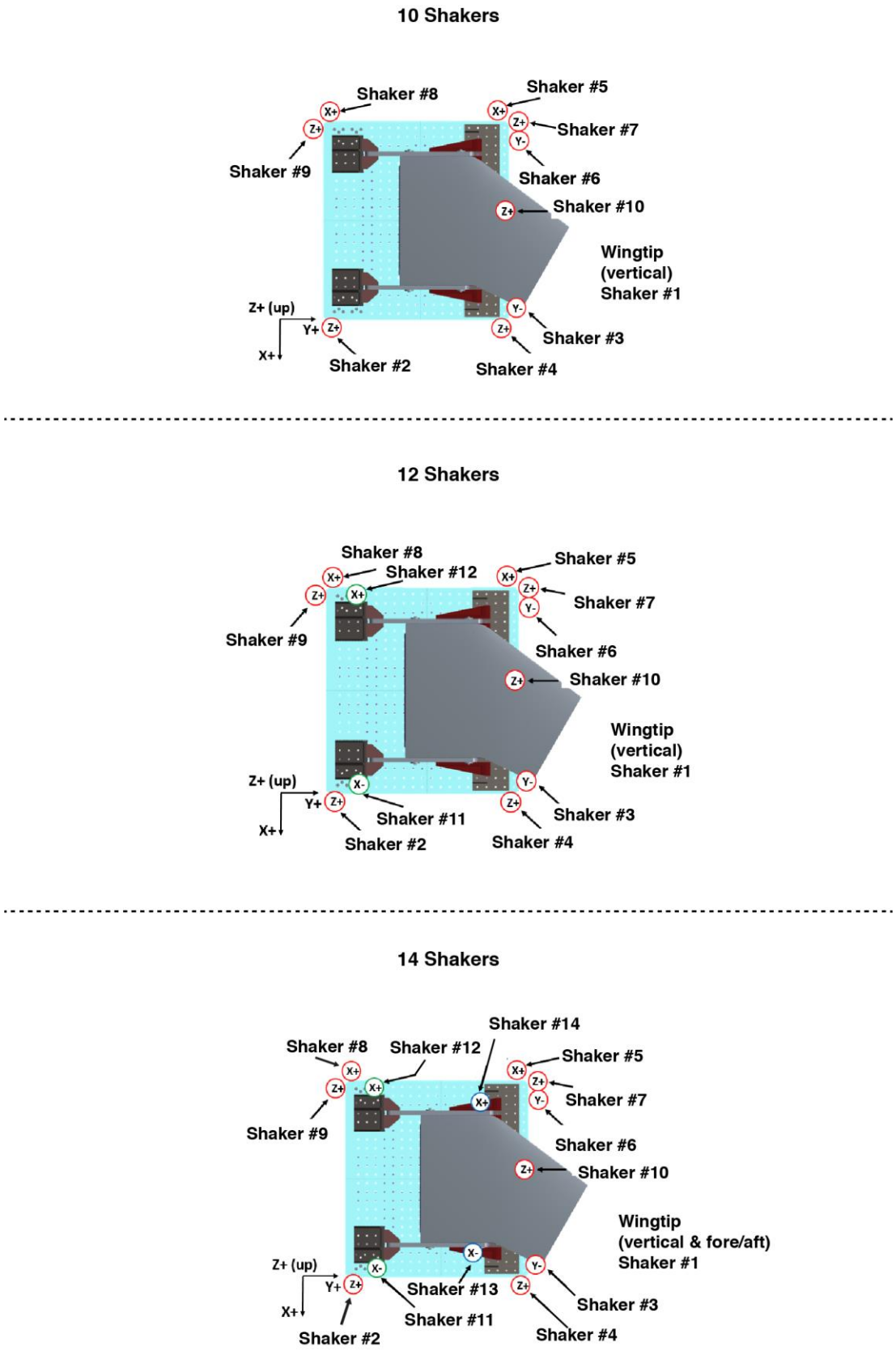

Figure 17: Shaker locations on the Passive Aeroelastic Tailored Wing

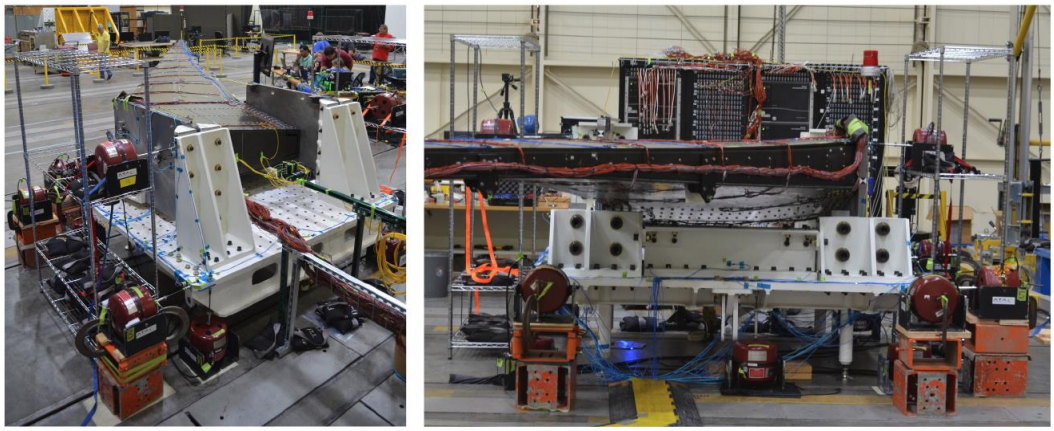

Figure 18: The Passive Aeroelastic Tailored Wing modal test shaker layout for the Fixed Base Correction Method

To compare the modal test FBC results with the above described shaker configurations to the FEM pre-test prediction results, analytical boundary conditions were placed on the FEM. Figure 19 shows how each FEM component was fully fixed. The FEM boundary conditions on all of the nodes that were rigid in all 6 DOF are shown in cyan. The fully-fixed FEM used for the pre-test modal analysis was the sum of the fixed boundary conditions on the reaction table, the aft two and forward two triangular brackets of the attachment hardware, and both wing reaction plates.

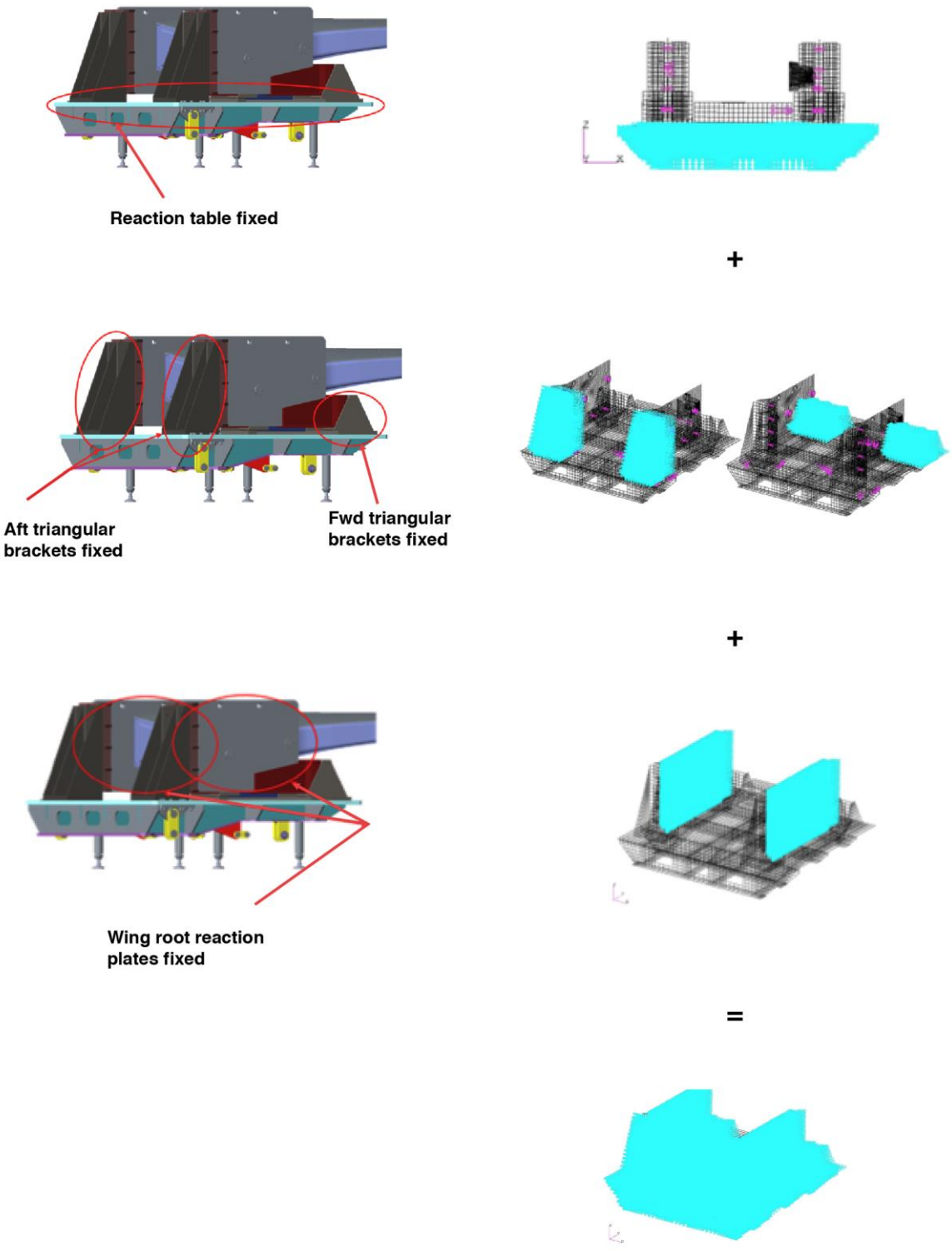

Figure 19: Finite element model fully-fixed boundary conditions

4 RESULTS

A total of 25 test runs were performed during the PAT Wing modal test using up to 14 shakers simultaneously to ensure the primary wing modes up to the W1T were cleanly extracted. The following PAT Wing modal results show that the FBC modes were successfully extracted using a total of 14 shakers.

4.1 Uncorrected Results

The uncorrected results using traditional modal testing techniques for the 10-shaker, 12-shaker, and 14-shaker configurations were all very similar. The 10-shaker and 12-shaker tests had vertical wingtip excitations, as did one of the 14-shaker tests. The other 14-shaker test had fore/aft wingtip excitation; the results of this test are shown in FEM/Test Cross MAC (modal assurance criterion) table 1. The main difference between the tests was that the WIT mode was difficult to pick up in tests that had vertical wingtip excitations rather than fore/aft wingtip excitations. The W1T mode was also difficult to pick up due to coupling with the Wing 5th Bending (W5B) mode and Wing 3rd Fore/Aft (W3F/A) mode. While all of the expected modes were captured up to W1T, only a few of the Cross MAC values were above 0.9, or 90 percent. The Cross MAC values also were not diagonal compared to a fully-fixed FEM, implying that the uncorrected test results did not accurately capture the correct mode shapes and frequencies. The blank terms in the Cross MAC are below 0.15, or 15 percent.

Table 1: Cross MAC of uncorrected results with 14 shakers

Uncorrected		FEM/Test Cross MAC Table													
14 Shakers		FEM Shapes													
Fore/Aft Wingtip Excitation		1	2	3	4	5	6	7	8	9	10	11	12	13	14
Fully Fixed Pretest FEM (Not Updated)		W1B	W2B	W1F/A	W3B	W2F/A	W4B	W5B (W1T)	W1T (W5B)	W3F/A	W6B	W2T	W2T (W4F/A)	W7B	W4F/A
	MAC	3.4	10.4	11.3	22.5	31.7	37.2	51.8	55.2	64.3	76.8	92.9	95.3	103.1	115.9
Test Shapes 1	W1B	3.5	0.99	0.30		0.16									
2	W1F/A (Base)	5.1			0.83										0.17
3	W2B (W1F/A, Base)	9.1	0.26	0.50	0.34	0.17									
4	W2B	10.1	0.32	0.98		0.40		0.19							
5	W2F/A (Base)	16.5			0.87		0.53								0.34
6	W3B (W2F/A, Base)	20.2		0.31		0.73		0.37							
7	W3B (Base)	22.0		0.28		0.88		0.35							
8	W2F/A (W4B, Base)	34.1			0.20	0.15	0.66	0.26		0.21					0.21
9	W4B (W2F/A, Base)	35.4				0.18	0.30	0.71			0.29					0.27
10	W5B (W1T, Base)	50.4						0.26	0.23	0.35						
11	W1T (Base)	56.5							0.70	0.30						
12	W3F/A (W1T, Base)	60.1					0.45				0.71					0.50
13	W6B (W3F/A, Base)	67.8					0.21				0.77					0.43
14	W6B (W4F/A, Base)	81.2										0.85			0.25	0.21
15	W4F/A (Base)	87.8									0.48					0.55
16	W4F/A (Base)	95.6									0.42					0.53
17	W2T (Base)	98.9											0.91	0.18		
18	W7B	N/A														

Many of the uncorrected mode shapes showed significant base motion, particularly the modes with wing fore/aft (F/A) and torsion (T) components. For example, a 9.1-Hz Wing 2nd Bending (W2B) mode coupled with the Wing 1st Fore/Aft (W1F/A) mode and base motion. The mode shape and undeflected wireframe is shown in figure 20. The bottom plate of the base is shown to have significant twisting motion as well as some rocking motion. The W2B mode is likely coupling with the W1F/A mode due to motion from the PAT Wing reaction plates; because this part of the base is not fixed, the base is coupling with wing modes. The mode disappears once the FBC method is applied, because the FBC method reduces the motion of the reaction plates as FBC base shakers are added.

Another challenge with the uncorrected test data was that there was a lot of coupling between modes in the 50- to 60-Hz range. This coupling can be discerned from table 1 (14-shaker uncorrected), as the W5B mode and the W3F/A mode (Modes 10 and 12, respectively) appear to have components of W1T and some base motion. The other

uncorrected tests (10 shakers and 12 shakers) also showed coupling between the W5B, W1T, and W3F/A modes; it was not possible to find a W1T mode from the 10-shaker and 12-shaker uncorrected tests. Utilizing the FBC method enabled decoupling these sorts of mode shapes.

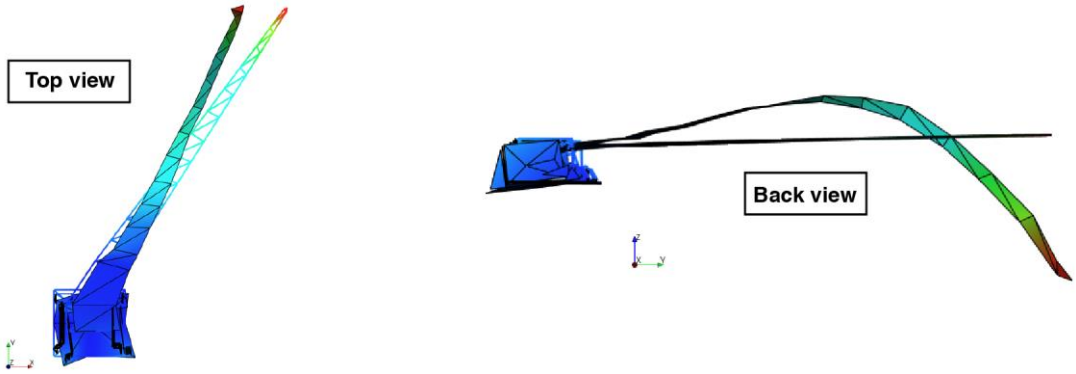

Figure 20: Uncorrected 9.1-Hz Wing 2nd Bending (Wing 1st Fore/Aft) mode with significant base motion (undeflected shape depicted by wireframe)

4.2 Fixed Base Corrected Results with 10 Shakers

A buildup testing approach was used to add shakers around the WLTF base to analytically fix it. The tests were initially started with 10 shakers, nine of which were on the WLTF reaction table; the 10th shaker was on the wingtip in the vertical direction as described above. The Cross MAC table for the 10-shaker FBC is table 2. As compared with the uncorrected Cross MAC in table 1, the first six mode shapes are now diagonal, indicating that the test results better match the FEM results. The Cross MAC results are actually better than expected; the first six flexible modes have very high (above 0.9, or 90 percent) diagonal Cross MAC values.

Table 2: Cross MAC of Fixed Base Corrected configuration with 10 shakers

Fixed Base Corrected			FEM/Test Cross MAC Table													
10 Shakers			FEM Shapes													
Vertical Wingtip Excitation			1	2	3	4	5	6	7	8	9	10	11	12	13	14
Fully Fixed Pretest FEM (Not Updated)			W1B	W2B	W1F/A	W3B	W2F/A	W4B	W5B (W1T)	W1T (W5B)	W3F/A	W6B	W2T	W2T (W4F/A)	W7B	W4F/A
		MAC	3.4	10.4	11.3	22.5	31.7	37.2	51.8	55.2	64.3	76.8	92.9	95.3	103.1	115.9
Test Shapes	1	W1B	3.5	0.99	0.31		0.16									
	2	W2B	10.2	0.33	0.99		0.40		0.18							
	3	W1F/A	10.7			0.94		0.24								0.22
	4	W3B	21.2		0.35		0.99		0.40							
	5	W2F/A	29.5			0.43		0.95			0.20					0.44
	6	W4B	35.1				0.33		0.95	0.20						
	7	W5B (W1T, Base)	52.1							0.26				0.15	0.32	
	8	W1T (W3F/A, Base)	55.6					0.27		0.20	0.41	0.32				0.21
	9	W3F/A (W1T, Base)	57.7			0.17		0.23		0.41		0.19				
	10	W6B (W3F/A, Base)	75.6									0.56	0.19			0.35
	11	W6B (W4F/A, Base)	78.9								0.16		0.81			0.29
	12	W4F/A (W2T, Base)	88.8									0.35				0.46
	13	W4F/A (W2T, Base)	95.9									0.33				0.53
	14	W2T (Base)	98.8										0.94	0.15		
	15	W7B (Base)	105.5									0.25			0.84	

Table 2 also shows that there are now only 15 modes up to the Wing 7th Bending (W7B) mode (as opposed to the 18 modes up to W7B in table 1), thus some of the redundant base modes were removed by applying FBC. The W7B mode was also able to be found by applying FBC; this mode was not found in the uncorrected Cross MAC table 1.

The Wing 1st Bending (W1B) and W2B modes did not show a lot of change after implementing FBC, which implies that the non-ideal modal test setup boundary condition was already stiff enough in the vertical direction to capture these modes. The FBC did, however, appear to significantly stiffen the W1F/A and Wing 2nd Fore/Aft (W2F/A) modes, increasing the Cross MAC values of these modes from approximately 0.85 (85 percent) to approximately 0.95 (95 percent), providing confidence that the FBC method is matching the test results to the FEM results.

The W1F/A and W2F/A mode shapes are shown in figure 21 comparing uncorrected and 10-shaker FBC test results. The FBC method significantly reduced, and almost eliminated, any base rotation, which can be seen as the blue lines in the insets in the figure. The wing shapes also show some improvement as well, since the FBC mode shapes have higher relative wingtip displacements at the wingtip than do the uncorrected mode shapes. Figure 21 also shows how applying the FBC method significantly stiffened the F/A modes, increasing the W1F/A frequency from 5 Hz to 11 Hz and increasing the W2F/A frequency from 17 Hz to 30 Hz. These results suggest that the FBC method has already significantly improved the quality of the GVT data gathered with only 10 shakers. The FBC method had the greatest effect on the F/A modes in the 10-shaker configuration.

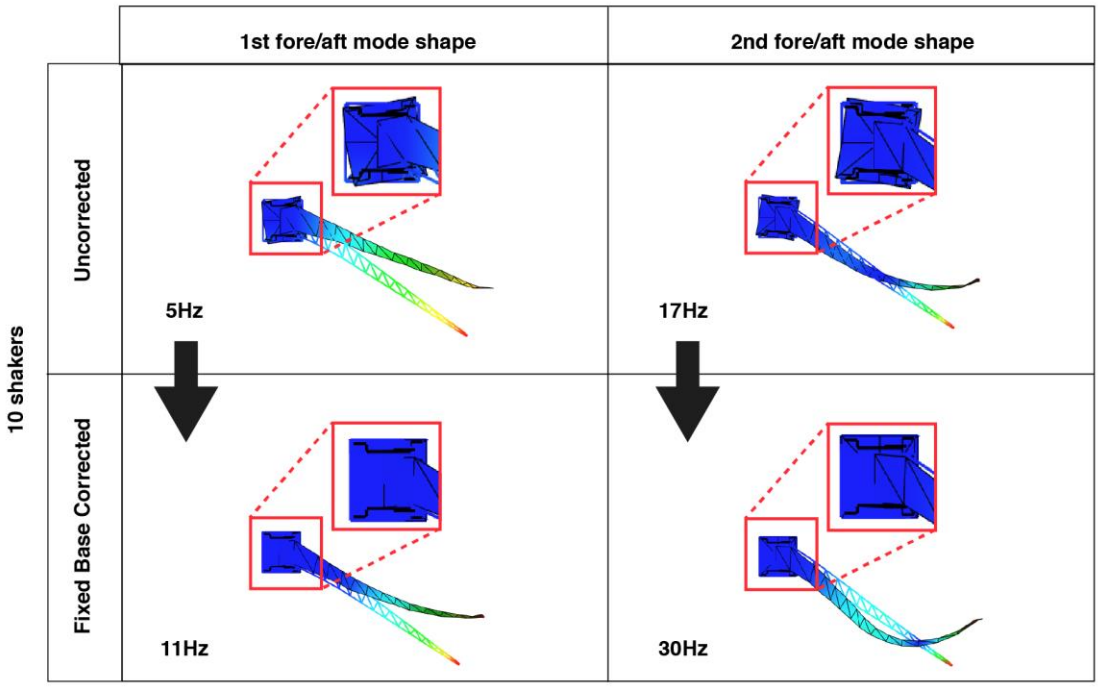

Figure 21: 10-shaker comparison of uncorrected versus Fixed Base Corrected for Fore/Aft modes (undeflected shape depicted by wireframe)

4.3 Fixed Base Corrected Results with 12 Shakers

After the 10-shaker FBC tests, an additional two shakers (shaker number 11 and number 12) were added on the attachment hardware known as the aft triangular brackets in the F/A direction, as seen in figure 17. These two shaker locations were chosen because the PAT Wing reaction plates showed significant F/A deflection. This method separated some of the coupled modes and added multiple more diagonal modes on the Cross MAC table, as can be seen in table 3. One highlight is that the W5B mode, W1T mode, and W3F/A mode were decoupled to some degree. This decoupling was very difficult to accomplish with only 10 shakers using the FBC method (table 2); it was also difficult to accomplish without using the FBC method (table 1). The W5B mode, the W1T mode, and the W3F/A mode finally could show up on the Cross MAC diagonal with values of 0.6 (60 percent) or better; it is likely that these values were not higher due to some remaining motion in the base. It is also notable that adding the two shakers reduced the number of modes from 15 (table 2) to 13 (table 3), again reducing the number of redundant base modes.

The 12-shaker FBC configuration was a significant improvement over the previous 10-shaker FBC configuration, which illustrates how crucial it is to the FBC method that an adequate number of shakers are added in the correct directions to fix the base modes up to the frequencies that are desired to be measured in the test article.

Table 3: Cross MAC of Fixed Base Corrected configuration with 12 shakers

Fixed Base Corrected			FEM/Test Cross MAC Table													
12 Shakers FBC			FEM Shapes													
Vertical Wingtip Excitation			1	2	3	4	5	6	7	8	9	10	11	12	13	14
Fully Fixed Pretest FEM (Not Updated)			W1B	W2B	W1F/A	W3B	W2F/A	W4B	W5B (W1T)	W1T (W5B)	W3F/A	W6B	W2T	W2T (W4F/A)	W7B	W4F/A
		MAC	3.4	10.4	11.3	22.5	31.7	37.2	51.8	55.2	64.3	76.8	92.9	95.3	103.1	115.9
Test Shapes	1	W1B	3.5	0.98	0.34		0.17									
	2	W2B	10.1	0.34	0.98		0.39		0.18							
	3	W1F/A	10.9			0.96		0.25								0.23
	4	W3B	21.3		0.35		0.99		0.41							
	5	W2F/A	29.7			0.42		0.95			0.19					0.44
	6	W4B	35.1				0.32		0.95	0.19						
	7	W5B (W1T)	52.2						0.19	0.60	0.30		0.23			
	8	W1T (W3F/A, Base)	57.1							0.42	0.59					
	9	W3F/A (Base)	58.2					0.47				0.81				0.47
	10	W6B (Base)	77.4									0.15	0.71		0.21	
	11	W4F/A (Base)	81.4					0.18				0.54	0.23			0.69
	12	W2T (Base)	98.5											0.92	0.18	
	13	W7B (Base)	106.8											0.18	0.71	

Adding the two F/A shakers also allowed the Wing 6th Bending (W6B) mode to show up on the Cross MAC diagonal. As can be seen in the 10-shaker FBC Cross MAC table (table 2), one of the test W6B modes appeared to couple with the FEM W3F/A mode due to the F/A motion of the PAT Wing reaction plates. Figure 22 compares the W6B mode shapes of the 10-shaker and 12-shaker FBC datasets to show how adding the two F/A shakers removed the W3F/A coupling by removing some of the base motion in the F/A direction.

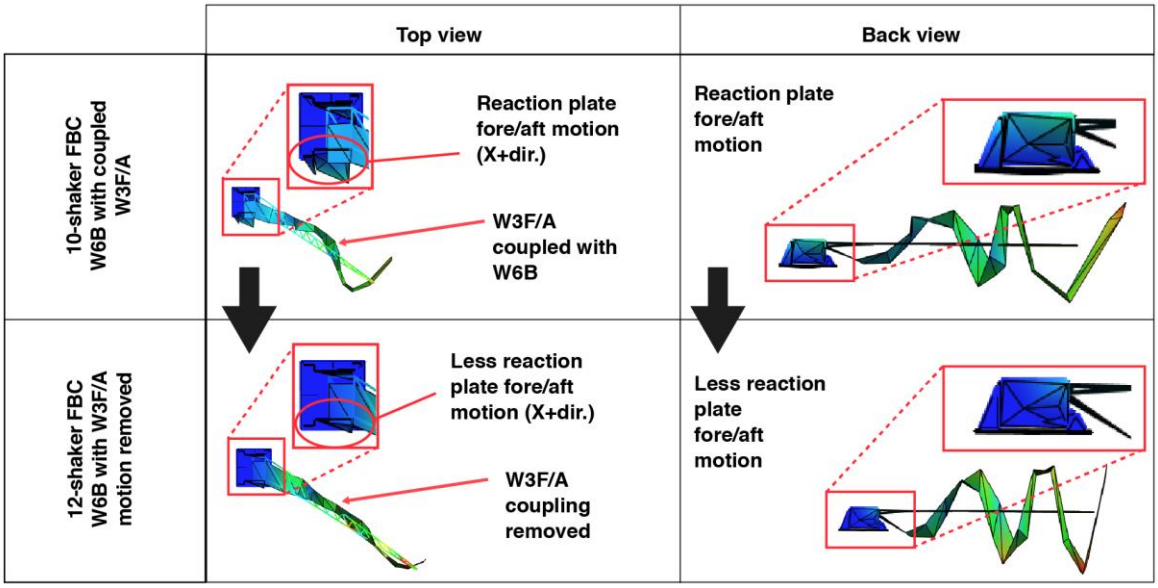

Figure 22: Comparison of Fixed Base Corrected Wing 6th Bending mode shapes with and without wing Fore/Aft coupling (10 versus 12 Shakers)

4.4 Fixed Base Corrected Results with 14 Shakers

Due to the remaining F/A motion in the base, two more shakers were added to the wing root reaction plates (figure 16 and figure 17) to remove most of the remaining base motion in the test article frequency range of interest. While the objective of the GVT was to accurately capture modes up to W1T, it was desired to examine several higher frequency modes to evaluate how well the FBC method could work with non-ideal modal boundary conditions.

There was not a significant change in the Cross MAC table between the 12-shaker and 14-shaker tests that used FBC. The 14-shaker FBC table is presented as table 4. The main difference is that the W6B mode showed improvement with the Cross MAC value increasing from 0.71 (71 percent) to 0.88 (88 percent). The W7B mode also improved from 0.71 (71 percent) to 0.82 (82 percent). It is promising that these modes improved, which shows how the FBC method continued to remove more base motion as more shakers are added in the correct directions and locations on the base.

Unfortunately, it continued to be difficult to improve the W1T mode and match it to the FEM W1T mode. The cause is probably the FEM W1T mode coupling with FEM W5B, so the test data W1T modes with less W5B coupling did not match as well as would be ideal.

Table 4: Cross MAC of Fixed Base Corrected configuration with 14 shakers

Fixed Base Corrected 14 Shakers Fore/Aft and Vertical Wingtip Excitation Fully Fixed Pretest FEM (Not Updated) Wingtip Excitation				FEM/Test Cross MAC Table FEM Shapes													
				1	2	3	4	5	6	7	8	9	10	11	12	13	14
				W1B	W2B	W1F/A	W3B	W2F/A	W4B	W5B (W1T)	W1T (W5B)	W3F/A	W6B	W2T	W2T (W4F/A)	W7B	W4F/A
			MAC	3.4	10.4	11.3	22.5	31.7	37.2	51.8	55.2	64.3	76.8	92.9	95.3	103.1	115.9
Test Shapes	1	Fore/Aft	W1B	3.6	0.99	0.33		0.17									
	2	Vertical	W2B	10.0	0.29	0.98		0.40		0.19							
	3	Fore/Aft	W1F/A	11.0			0.94		0.24								0.21
	4	Fore/Aft	W3B	21.2		0.34		0.99		0.41							
	5	Fore/Aft	W2F/A	30.2			0.41		0.96			0.18					0.43
	6	Fore/AFt	W4B	35.2				0.32		0.95		0.20					
	7	Vertical	W5B (W1T)	52.2						0.20	0.69	0.21		0.21			
	8	Vertical	W1T	56.4							0.40	0.57					
	9	Vertical	W3F/A (W1T)	59.1					0.46			0.15	0.73				0.46
	10	Vertical	W6B (Base)	77.4										0.88		0.23	
	11	Vertical	W4F/A (W2T, Base)	88.6			0.16		0.21				0.50		0.17	0.17		0.70
	12	Vertical	W2T (Base)	98.6										0.90	0.20		
	13	Vertical	W7B (Base)	106.4									0.17			0.82	

The use of the FBC method significantly reduced the difference between the test frequencies and the fully-fixed FEM frequencies, as can be seen in table 5. The frequencies with a percent difference under five percent are shaded green, the frequencies with a percent difference under than ten percent are shaded orange, and the frequencies with a percent difference above ten percent are shaded red. Only the modes up to the W1T test objective are shown. Five of the uncorrected redundant base modes were excluded from this table in order to simplify the comparison between uncorrected and FBC. The F/A modes benefitted the most from correction. The W1F/A mode percent difference dropped by about fifty percent, which also corresponded to a large frequency shift from 5 Hz to 11 Hz. Modes other than F/A did not exhibit frequencies that looked significantly different. The main thing that the FBC method improved for these modes was cleaning up the test wing mode shapes to better match the FEM mode shapes, which is reflected by the Cross MAC table values increasing as more shakers were added while using the FBC method. Some values, however, did not increase significantly due to remaining small amounts of base motion.

Applying the FBC method can either increase or decrease the frequency of an uncorrected mode. If there is an inertial boundary condition effect (which is common with shake tables), the frequency tends to decrease as FBC is

applied. If there is a stiffness boundary condition effect (which is common with static structures), the frequency tends to increase as FBC is applied.

Table 5: Frequency percent difference with respect to finite element model between 14-shaker uncorrected and 14-shaker Fixed Base Corrected

Mode #	Mode Description	Frequency (Hz)			% Difference to FEM Frequency	
		FEM	14-Shaker Uncorrected	14-Shaker FBC	14-Shaker Uncorrected	14-Shaker FBC
1	W1B	3.4	3.5	3.6	3%	5%
2	W2B	10.4	10.1	10.0	-3%	-4%
3	W1F/A	11.3	5.1	11.0	-55%	-3%
4	W3B	22.5	22.0	21.2	-2%	-6%
5	W2F/A	31.7	16.5	30.2	-48%	-5%
6	W4B	37.2	35.4	35.2	-5%	-5%
7	W5B (W1T)	51.8	50.4	52.2	-3%	1%
8	W1T	55.2	56.5	56.4	2%	2%

A comparison of the W7B modes between the 12-shaker and 14-shaker FBC tests shows a little improvement in the base stiffness, as can be seen in figure 23. While both modes were relatively clean after adding so many base shakers, the 14-shaker configuration reduced the F/A motion of the reaction plates which reduced the Wing 4th Fore/Aft (W4F/A) motion that the W7B mode shapes were experiencing.

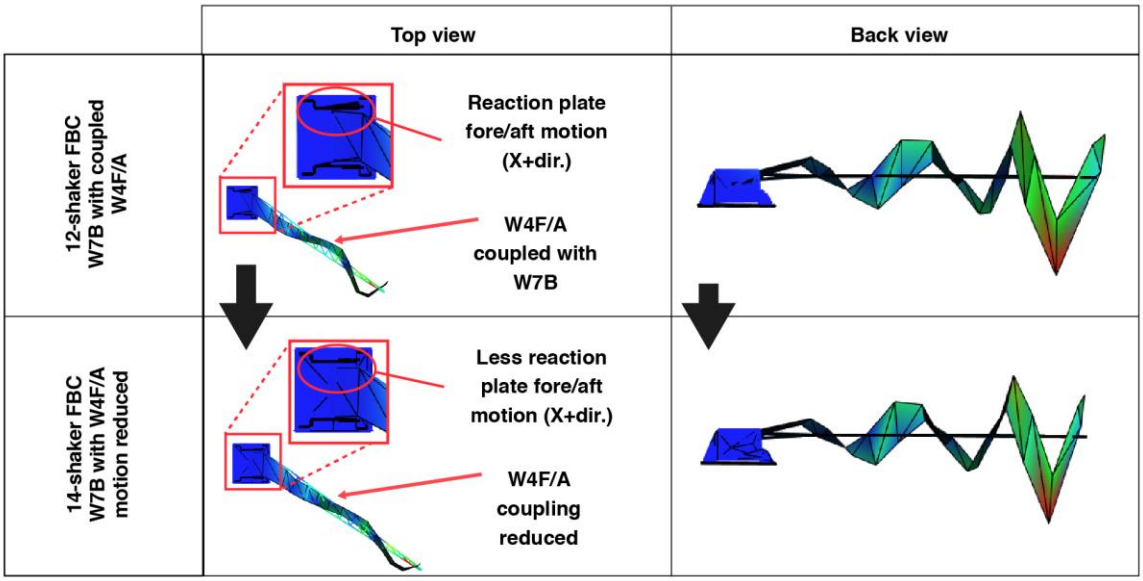

Figure 23: Comparison of Fixed Base Corrected Wing 7th Bending mode shapes from 12-shaker versus 14-shaker: Wing 4th Fore/Aft coupling reduced

One of the primary benefits of applying the FBC method was reducing the base motion that coupled with various wing modes. One example was the W4F/A mode. In the uncorrected post-processing Mode Indicator Functions (MIFs), there were two peaks associated with W4F/A: one at 87 Hz, and the other at 95 Hz. Both mode shapes looked similar and the MIF peaks were about the same size, making it difficult to determine which was the true W4F/A mode. In contrast, there was only one MIF peak associated with W4F/A in the FBC post-processing at 88 Hz, as can be seen in figure 24.

In future tests, FBC results could potentially be improved by adding more accelerometers on the wing and base. There could also be more optimization performed when choosing locations for the base shakers. The PAT Wing GVT shows that the FBC method is promising, although more research is needed for aeronautics applications.

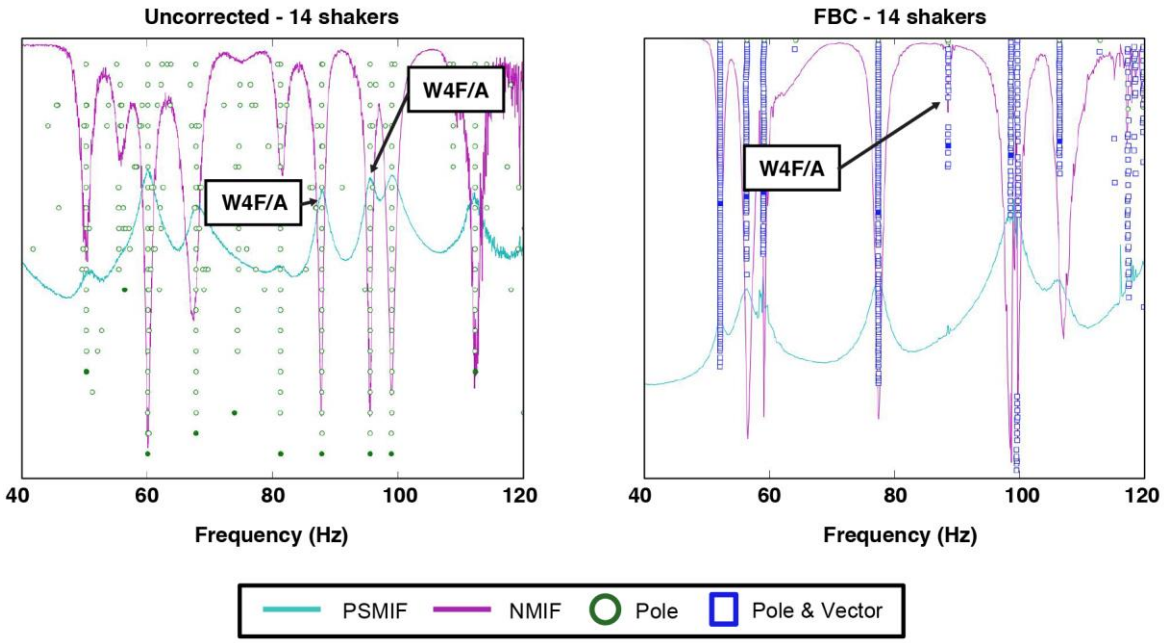

Figure 24: Comparison of mode indicator functions for 14-shaker uncorrected versus 14-shaker Fixed Base Corrected

All of the uncorrected 14-shaker mode shapes can be seen in figure 25. Only an abbreviated version of the mode shape names is shown in figure 25; the complete uncorrected test mode shape names can be seen in table 1.
All of the FBC 14-shaker mode shapes can be seen in figure 26.

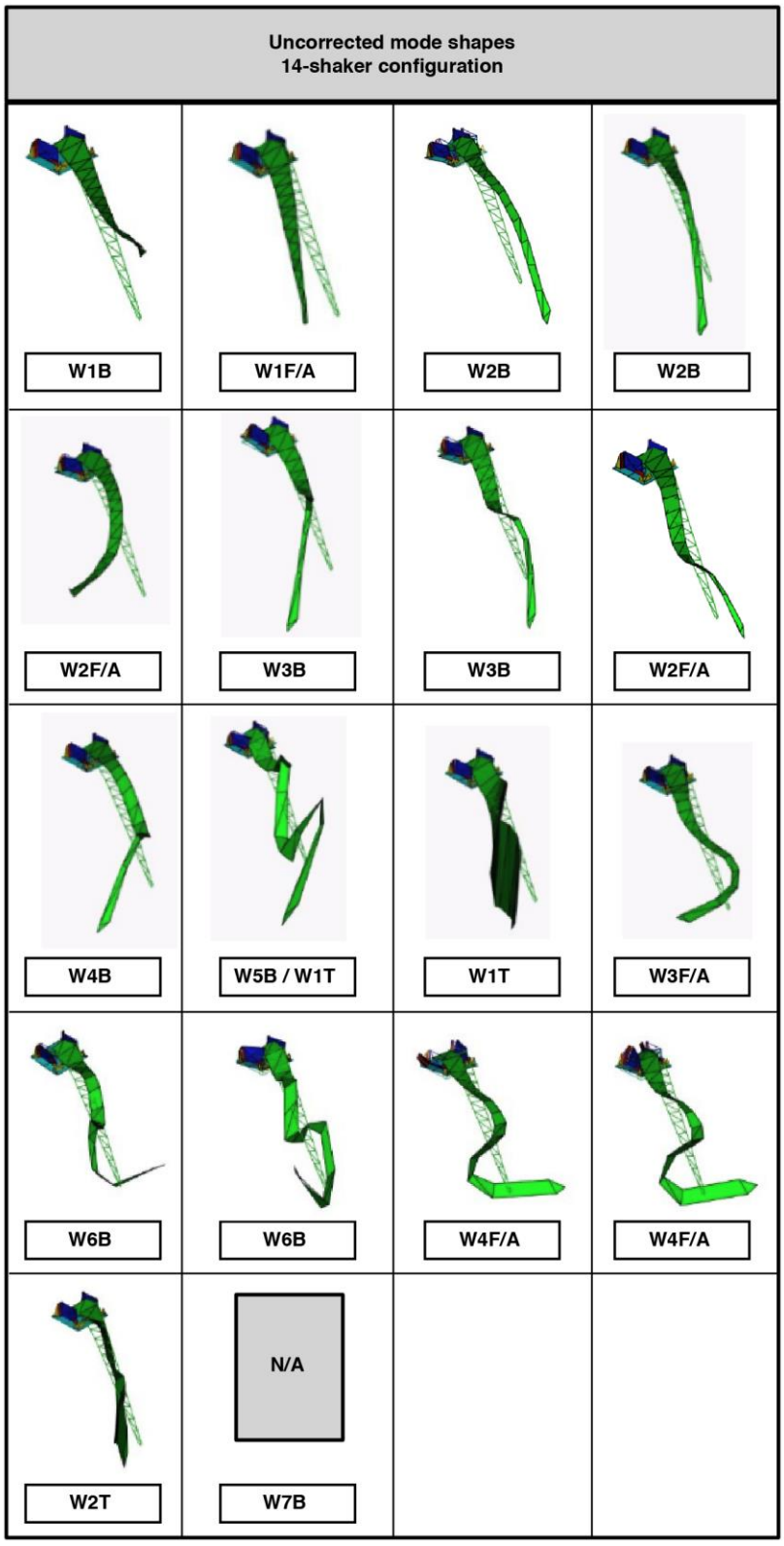

Figure 25: Isometric mode shape pictures: uncorrected 14-shaker configuration

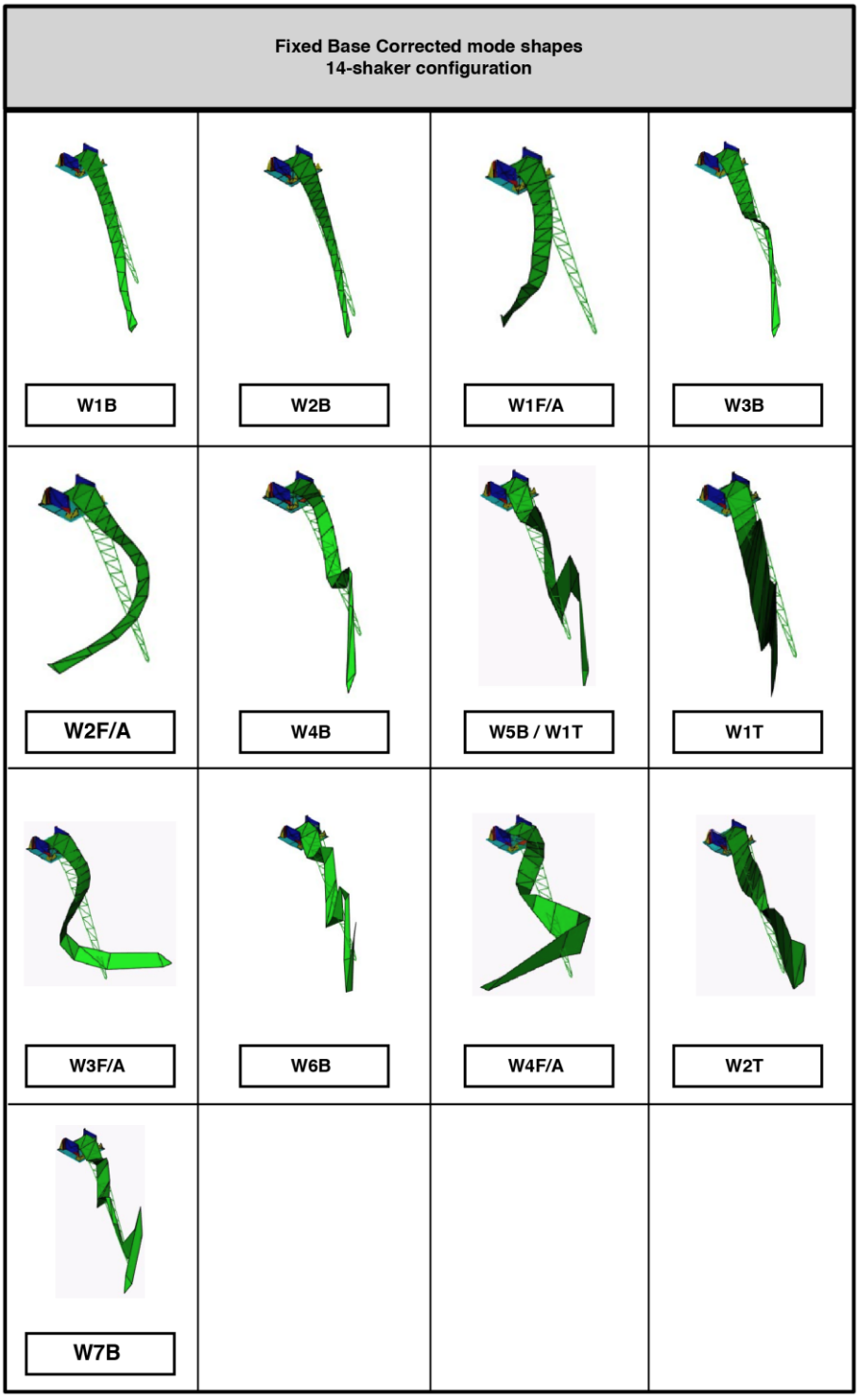

Figure 26: Isometric mode shape pictures: fixed base corrected 14-shaker configuration

SUMMARY

Passive Aeroelastic Tailored Wing ground vibration test results show the feasibility of using the Fixed Base Correction (FBC) method to decouple the wing and test fixture modes for a long flexible wing mounted to a

dynamically active static test fixture. The test frequencies and mode shapes of the wing better matched fixed boundary condition finite element model predictions by using this method. The FBC technique is implemented by applying an excitation to the desired "fixed" boundary hardware with multiple independent sources (that is, shakers) where there are at least as many independent sources as there are independent boundary deformations in the test article frequency range of interest. The FBC method then uses the shaker boundary accelerations (measured by seismic accelerometers) as independent references when calculating frequency response functions. This FBC method has the potential to change how modal testing is traditionally performed and can save money and schedule time by eliminating an independent setup for modal testing. The FBC results also produce test results with reliable and comparable boundary conditions to replicate in and compare with analytical models.

ACKNOWLEDGEMENTS

The authors gratefully acknowledge the NASA Advanced Air Transport Technology (AATT) project for the funding support to accomplish the Passive Aeroelastic Tailored (PAT) Wing modal testing. The PAT Wing is under the AATT project of the NASA Advanced Air Vehicles Program (AAVP). We also thank the NASA Armstrong Flight Loads Laboratory technicians and mechanics for their assistance in setting up and performing the ground vibration test. The NASA authors acknowledge Aurora Flight Sciences for designing and fabricating the towed-steered wingbox, and ATA Engineering, Inc. for assisting with the testing and guidance through the post-test data analysis using the fixed base correction method.

REFERENCES

[1] Armstrong Flight Loads Laboratory, https://www.nasa.gov/centers/armstrong/research/Facilities/FLL, accessed October 17, 2019.

[2] Brooks, T. R., Martins, J. R. R. A, and Kennedy, G. J., "High-fidelity Aerostructural Optimization of a High Aspect Ratio Tow-steered Wing," AIAA-2016-1179, 2016.

[3] Brooks, T. R., Martins, J. R. R. A., and Kennedy, G. A., "High-fidelity Multipoint Aerostructural Optimization of a High Aspect Ratio Tow-steered Composite Wing," AIAA-2017-1350, 2017.

[4] Brooks, T. R., Kenway, G. K W., and Martins, J. R. R. A., "Benchmark Aerostructural Models for the Study of Transonic Aircraft Wings," *AIAA Journal*, Vol. 56, No. 7, July 2018.

[5] Spivey, N., Miller, K. Saltzman, R., and Napolitano, K., "Modal Testing of a Flexible Wing on a Dynamically Active Test Fixture Using the Fixed Base Correction Method," IFASD 2019-108, 2019.

[6] Crowley, J. R., Klosterman, A. L., Rocklin, G. T., and Vold, H., "Direct Structural Modification Using Frequency Response Functions," *Proceedings of the 2nd International Modal Analysis Conference*, Orlando, Florida, pp. 58-65, 1984.

[7] Beliveau, J. G., Vigneron, F. R., Soucy, Y., and Draisey. S., "Modal Parameter Estimation from Base Excitation," *Journal of Sound and Vibration*, Vol. 107(3), pp. 435-449, 1986.

[8] Imregun, M., Robb, D. A., and Ewins, D. J., "Structural Modification and Coupling Dynamic Analysis Using Measured FRF Data," *Proceedings of the 5th International Modal Analysis Conference*, London, England, pp. 1136-1141, 1987.

[9] Carne, T.G., Martinez, D. R., and Nord, A. R., "A Comparison of Fixed-Base and Driven-Base Modal Testing of an Electronics Package," *Proceedings of the 7th International Modal Analysis Conference*, Las Vegas, Nevada, pp. 672-679, 1989.

[10] Fullekrug, U. "Determination of Effective Masses and Modal Masses from Base-Driven Tests," *Proceedings of the 14th International Modal Analysis Conference*, Dearborn, Michigan, pp. 671-681, 1996.

[11] Sinapius, J. M., "Identification of Free and Fixed Interface Normal Modes by Base Excitation," *Proceedings of the 14th International Modal Analysis Conference*, Dearborn, Michigan, pp. 23-31, 1996.

[12] Mayes, R. L., and Bridgers, L. D., "Extracting Fixed Base Modal Models from Vibration Tests on Flexible Tables," *27th Conference and Exposition on Structural Dynamic 2009 (IMAC XXVII), Vol. 2,* Orlando, Florida, pp. 957-970, 2009.

[13] Allen, M. S, and Mayes, R. L., "Recent Advances to Estimation of Fixed-Interface Modal Models using Dynamic Substructuring," *Dynamics of Coupled Structures, Volume 4, Proceedings of the 36th IMAC, A Conference and Exposition on Structural Dynamics,* Orlando, Florida, pp. 157-170, 2018.

[14] Napolitano, K. L., and Yoder, N. C., "Fixed Base FRF Using Boundary Measurements as References - Analytical Derivation," *Topics in Modal Analysis I, Volume 5, Proceedings of the 30th IMAC, A Conference on Structural Dynamics,* Jacksonville, Florida, pp. 299-308, 2012.

[15] Mayes, R. L., Rohe, D. P., and Blecke. J., "Extending the Frequency Band for Fixed Base Modal Analysis on a Vibration Slip Table," *Topics in Experimental Dynamic Substructuring, Volume 2, Proceedings of the 31st IMAC, A Conference on Structural Dynamics,* Garden Grove, California pp. 287-297, 2013.

[16] Napolitano, K. L., Yoder, N. C., and Fladung, W. A., "Extraction of Fixed-Base Modes of a Structure Mounted on a Shake Table," *Topics in Experimental Dynamic Substructuring, Volume 2, Proceedings of the 31st IMAC, A Conference on Structural Dynamics,* Garden Grove, California pp. 299-309, 2013.

[17] Napolitano, K. L., "Fixing Degrees of Freedom of an Aluminum Beam by Using Accelerometers as References," *Proceedings of the 37th IMAC,* Orlando, Florida, pp. 53-60, 2019.

[18] Yoder, N. C., and Napolitano, K. L., "Fixed Base FRF using Boundary Measurements as References - Experimental Results," *Topics in Modal Analysis I, Volume 5, Proceedings of the 30th IMAC, A Conference on Structural Dynamics,* Jacksonville, Florida, pp. 309-317, 2012.

[19] Napolitano, K. L., "Using Singular Value Decomposition to Estimate Frequency Response Functions," *Topics in Modal Analysis & Testing, Volume 10, Proceedings of the 34th IMAC,* San Diego, California, pp. 27-43, 2016.